

ISTITUTO NAZIONALE DI RICERCA METROLOGICA Repository Istituzionale

Metrological characterization of an hexapod-shaped Multicomponent Force Transducer

This is the author's submitted version of the contribution published as:
Original Metrological characterization of an hexapod-shaped Multicomponent Force Transducer / Genta, G.; Germak, ALESSANDRO FRANCO LIDIA; Barbato, G.; Levi, R In: MEASUREMENT ISSN 0263-2241 78:(2016), pp. 202-206. [10.1016/j.measurement.2015.09.054]
Availability: This version is available at: 11696/33588 since: 2021-03-08T19:25:30Z
Publisher: Elsevier
Published DOI:10.1016/j.measurement.2015.09.054
Terms of use:
This article is made available under terms and conditions as specified in the corresponding bibliographic description in the repository
Publisher copyright

(Article begins on next page)

Metrological characterization of an hexapod-shaped Multicomponent Force Transducer

Gianfranco Genta ^{a, f)}, Alessandro Germak ^b, Giulio Barbato ^a, Raffaello Levi ^a

1. Introduction

The present work was originated by a specific industrial request, concerning performances of coil springs in railway carriage suspension. Spring deflection under axial load entails also, as a rule, a side component, originating a transversal force and/or displacement, see (Fig. 1). Such a displacement (orthogonality error under load) is currently denoted by the French term "Chasse" [1].

These coil springs are usually checked on large capacity dedicated testing machines, relying upon hydraulic or mechanical devices for force generation. Machine platens usually do not allow side displacement; therefore "Chasse" may not be measured directly. Furthermore it is worth remarking that what really matters is preventing carriage's side displacement due to spring deflection. Therefore in railways engineering practice coil springs are assembled, and oriented, in carriage suspension aiming at offsetting side displacement, by producing under deflection side forces opposing each other. In order to achieve such result, knowledge of side force under axial load, and its orientation, is a prerequisite.

However technical specifications [1] mandate formal evaluation of the displacement "Chasse". A measurement strategy was adopted, based upon identifying side force direction under load, and rotate the spring under test around its vertical axis in order to align the direction of "Chasse" with that of a sliding table, set upon testing machine platen. The sliding table is then moved as required to produce zero side force, the corresponding displacement being taken as a measure of "Chasse".

A device is therefore required, capable of measuring modulus and direction of both axial and side force, the former corresponding with spring axis. While a three-component Multicomponent Force Transducer (MFT) — capable of measuring F_x , F_y and F_z —would fit the bill, knowledge also of moments (M_x , M_y , M_z) offers substantial advantages, in terms of better identification of calibration equations.

Substantial experience accumulated at INRiM on development of multicomponent force measurement devices and related calibration rigs [2] suggested design and development of an *ad hoc* MFT. Capacity of MFTs previously

^a DIGEP, Politecnico di Torino, Corso Duca degli Abruzzi 24, 10129 Torino, Italy

^b Istituto Nazionale di Ricerca Metrologica (INRiM), Strada delle Cacce 91, 10135 Torino, Italy

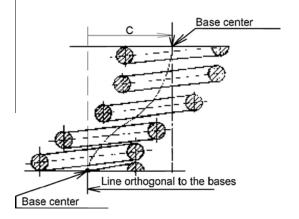


Fig. 1. "Chasse" C defined as side displacement due to axial load.

developed at INRiM ranges from few newtons to hundreds of kilonewtons, with different configurations, e.g. integral or built-up. Typical applications covered control of parasitic components in force standard calibration machines, verification of material testing machines, robotics, and cutting force evaluation in machining research [3].

A large capacity six component MFT, hexapod shaped, was developed for the task at hand by INRiM for a firm operating in the field of mechanical testing. Such a structure, typical of six degrees of freedom displacement devices (Stewart platforms), was previously exploited by INRiM in low capacity MFTs, particularly in robotics [4,5].

Mandated uncertainties for the case at hand are 1% on side force measurement, and class 1 of ISO 7500-1:2004 [6] on axial force measurement.

2. Description of the MFT

The MFT has an axial force capacity of $200 \, \mathrm{kN}$ and of $30 \, \mathrm{kN}$ for transversal force. Its built-up design is made up by six Uniaxial Force Transducers (UFTs) individually calibrated on a deadweight force standard machine. Their calibration equations are taken into account to get, in terms of the six UFT outputs O_i , the corresponding measures $F_{m,i}$ of the forces F_i acting on each arm $(i=1,\ldots,6)$.

Every UFT installed into the hexapod structure is decoupled by integral elastic hinges at both ends (Fig. 2),

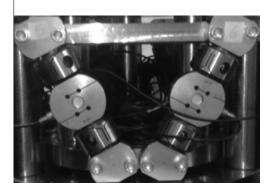


Fig. 2. Two of the six Uniaxial Force Transducers (UFTs) decoupled by integral elastic hinges at both ends.

substantially eliminating spurious components, which might otherwise affect measurements [7]. Such a structure (Fig. 3) enables measuring three force components (transversal, F_x and F_y , and axial, F_z), and three moment components, (tilting, M_x and M_y , and torsion, M_z). Theoretical values of the three force and three moment components may be calculated in terms of nominal MFT geometry, and the relevant uncertainties estimated a priori by assuming a set of deviations from the geometry thereof.

Since this work covers mainly experimental evaluation of metrological characteristics of MFT, where actual geometry is directly taken into account, only uncertainty contributions due to reproducibility are considered.

3. Calibration of the MFT

Transducer design caters for both comprehensive initial calibration and a simpler procedure for maintenance over time. Within the specified range of combinations of applied forces and moments, all the UFTs are loaded in tension only.

The first calibration is useful to determine both the effects of the geometry of the structure and the sensitivities of the UFTs. Since the MFT, installed in a spring testing machine (Fig. 4), is not moved over time, the geometry is not subject to significant changes. Thus, the subsequent calibrations are restricted only to the evaluation of the variation over time of sensitivities of the UFTs by applying known values of vertical components F_z .

INRiM was tasked with the first calibration of the MFT in order to have traceable measurements with a proper uncertainty evaluation [8]. A well-established metrological approach [3] asserts that forces must be applied both independently and in combination to assess cross sensitivity among output channels (if any). Testing procedure strictly requires only calibration for F_x and F_z .

Calibration for F_z was performed on the primary INRiM deadweights standard machine with a capacity of 1 MN, following the international calibration procedure; results



Fig. 3. Layout of the hexapod-shaped Multicomponent Force Transducer (MFT).

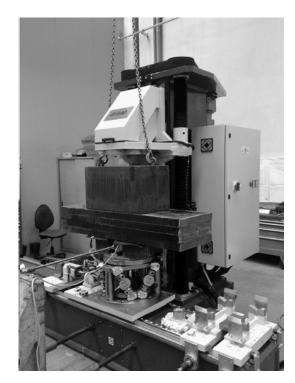


Fig. 4. Calibration set-up on the spring testing machine; transversal force applied by a rod.

showed the MFT being in class 00 according to ISO 376:2011 [9]. Calibration of F_x was instead performed with the MFT installed on the spring testing machine, evaluating the all-important cross sensitivity with F_z , generated using deadweights, transversal forces being applied by mechanical devices and measured with a calibrated UFT (Fig. 4).

4. Analysis of calibration results

Using the described calibration set-up (Fig. 4), transversal forces and axial forces were applied. Given the target of uncertainties (mentioned in Section 1), and in the light of results obtained in preliminary tests, a restricted experimental plan with only two levels of F_z and few levels of F_x was deemed adequate and performed accordingly.

Taking into account the availability of deadweights in the site of calibration, two levels of F_z were selected, namely about 14 kN and 23 kN. With these levels of force, values of F_x ranging up to 3 kN and 5 kN respectively were chosen, so as to apply only tensile force to each UFT. By applying component F_x an associated tilting moment M_y is also generated. Applied components and corresponding force and moment measurement results are shown, respectively, in Table 1 and 2.

While F_x is expected to be related mainly to the output $F_{m,x}$, and F_z to the output $F_{m,z}$, owing to cross-sensitivity the presence of other terms was anticipated. Linear regression analysis [10] was applied to get an empirical mathematical model linking the applied components to the MFT outputs. In particular, Best Subset Regression [11] was adopted to identify parsimonious models for F_x and F_z by considering

Table 1 Applied components.

No	F_x/kN	F ₂ /kN	$M_y/(N m)$
1 2	0.000 0.000	0.000 -22.969	0.0 0.0
3	0.563	-22.969	-281.6
4	1.050	-22.969	-524.8
5	2.019	-22.969	-1009.5
6	4.045	-22.969	-2022.4
7	4.992	-22.969	-2495.9
8	0.000	-14.066	0.0
9	0.528	-14.066	-264.1
10	0.996	-14.066	-498.2
11	2.028	-14.066	-1014.2
12	3.006	-14.066	-1503.0

Table 2
Measured forces and moments corresponding to the applied components shown in Table 1.

No	$F_{m,x}/\mathrm{k}\mathrm{N}$	$F_{m,y}/kN$	$F_{m,z}/kN$	$M_{m,x}/(N m)$	$M_{m,y}/(N m)$	$M_{m,2}/(N m)$
1	0.000	0.000	0.000	0.0	0.0	0.0
2	0.000	0.000	-22.969	0.0	0.0	0.0
3	0.520	0.001	-22.959	76.7	-279.4	-0.4
4	0.962	0.004	-22.959	69.7	-517.7	0.4
5	1.850	0.016	-22.952	52.9	-995.7	-0.4
6	3.699	0.049	-22.931	4.5	-1996.3	-0.4
7	4.563	0.070	-22.937	-33.0	-2465.2	-4.7
8	0.000	0.000	-14.066	0.0	0.0	0.0
9	0.483	0.041	-14.134	-11.7	-244.6	7.7
10	0.914	0.044	-14.134	-16.3	-474.5	8.4
11	1.862	0.059	-14.121	-38.7	-982.4	7.7
12	2.759	0.075	-14.111	-62.8	-1462.2	5.1

Table 3 Standard deviations of equation coefficients.

Coefficient	Std. dev.
a h	7.56×10^{-4} 6.73×10^{-3} m ⁻¹
c	$3.52 \times 10^{-5} \mathrm{kN^{-1}}$
d e	2.65×10^{-3} 1.19×10^{-1}
f	1.82 x 10 ⁻⁴

all possible combinations of predictor variables (F, F_{m,x}, F_{m,y}.

 $F_{m,z}$, $M_{m,x}$, $M_{m,y}$ and $M_{m,z}$). The limited number of experiments allowed only considering models up to first order with interactions. This is acceptable considering the linearity characteristic of the UFTs. The following equations were obtained; for the transversal force:

$$F_x \stackrel{1}{\cancel{4}} a \cdot F_{m,x} \triangleright b \cdot M_{m,x} \triangleright c \cdot F_{m,x} \cdot F_{m,z} \triangleright e_{Fx}$$
 ð1Þ

where a = 1.08, $b = -6.16 \times 10^{-2} \text{ m}^{-1}$ and $c = -6.04 \times 10^{-4} \text{ k.N}^{-1}$, while for the axial force:

$$F_z \not A d \cdot F_{m,x} \triangleright e \cdot F_{m,y} \triangleright f \cdot F_{m,z} \triangleright \mathbf{e}_{Fz}$$
 ð2Þ

where $d = -3.90 \times 10^{-2}$, e = 2.00 and f = 1.00. The terms Θ_{Fx} and Θ_{Fx} take into account of random errors.

The models include as significant terms for F_x besides $F_{m,x}$, also $M_{m,x}$ and the interaction term $F_{m,x} \cdot F_{m,z}$, while

Table 4 Uncertainty table for the transversal force F_x (expressed in kilonewton).

x_j		$u(x_j)$ c_j		$u_j^2 (F_x)$	m _j	$u_{j}^{4}(F)/\mathbf{m}_{j}$
Symbol	Value					
а	1.1	7.6 x 10 ⁻⁴	3.0	5.1 x 10 ⁻⁶	9	2.9 x 10 ⁻¹²
b	-6.2×10^{-2}	6.7×10^{-3}	1.0×10^{-1}	4.5×10^{-7}	9	2.3×10^{-14}
С	-6.0×10^{-4}	3.5×10^{-5}	-4.2×10^{1}	2.2×10^{-6}	9	5.3×10^{-13}
$F_{m,x}$	3	1.2×10^{-4}	1.1	1.6×10^{-8}	100	2.4×10^{-18}
$F_{m,z}$	-14	1.2×10^{-4}	-1.8×10^{-3}	4.4×10^{-14}	100	1.9×10^{-29}
$M_{m,x}$	0.1	2.9×10^{-5}	-6.2×10^{-2}	3.2×10^{-12}	100	1.0×10^{-25}
$\mathbf{e}_{\scriptscriptstyle Fx}$	0	8.1×10^{-4}	1.0	6.6×10^{-7}	9	4.8×10^{-14}
F_x	3.3		$u^2(F_x)$	8.5 x 10 ⁻⁶	R	3.5 x 10 ⁻¹²
			$u(F_x)$	2.9×10^{-3}	m _{ir}	20
			p	95%	-	
			$t_p \left(\mathbf{m}_{Fx} \right)$	2.1		
			$U(F_x)$	6.1×10^{-3}		
			$W(F_x)$	0.19%		

the corresponding model for F_z includes, besides $F_{m,z}$, also $F_{m,x}$ and $F_{m,y}$. The significant contribution of the interaction $F_{m,x} \cdot F_{m,z}$ in Eq. (1) underlines the advantages of exploiting a full six-component MFT even when measurement of only two components is required.

Expanded uncertainty associated to the values of F_x and F_z was evaluated in terms of estimated mathematical models [12,13]. Main factors were, specifically, considered:

- the effects of the deviation from the nominal geometry were evaluated by means of the regression coefficients, and the relevant standard uncertainties were estimated as the corresponding standard deviations obtained in the performed linear regressions (Table 3);
- the effects of resolution of input quantities F_i shall be specifically considered, as usual in the application of GUM [8]. For the proposed models, being measured forces and moments directly used, the corresponding effect of F_i resolution was propagated obtaining respectively a standard uncertainty of 0.12 N and 0.03 N m;
- the effects of random factors \(\mathbb{e}_{Fx}\) and \(\mathbb{e}_{Fz}\), representing
 the measurement reproducibility, are estimated by considering the standard deviation of regression residuals,
 which results respectively 0.8 N for \(F_x\) and 7.6 N for \(F_z\).

The uncertainty evaluation according to GUM [8] and PUMA method (described in ISO 14253-2:2011 [14]) may be properly organized in a tabular format, with reference to EA-4/02M:2013 [15]. A small modification from this format has been introduced by substituting standard deviations with variances; thus managing additive quantities which can be compared more easily. In this way, individual contributions to variance of output quantity F_x are shown for a specific working condition in Table 4.

Symbols of independent variables appearing in the mathematical model and their values are written down in column x_j . Entries in column $u(x_j)$ are the standard uncertainties for each contribution, while values in column \mathbf{m}_j represent the degrees of freedom. Coefficients of sensitivity c_j may be evaluated either by partial derivation, or numerically, and eventually contributions $u_j^2(F)$ of variance of dependent variable F_x can be calculated. By taking into account all these information, it is possible to get the expanded uncertainty $U(F_x)$.

The same type of calculation was performed for F_z . In this way, it is obtained a relative expanded uncertainty of about 0.2% both for F_x and for F_z . These values resulted to be nearly constant, in the considered experimental conditions, when ratio between F_x and F_z is about one fifth. However, when this ratio decreases, the relative expanded uncertainty on F_z also decreases till about 0.04%.

5. Conclusion

A Multicomponent Force Transducer (MFT) was developed by INRiM for a specific request in railway industry. While testing procedure strictly required only calibration for F_x and F_z , INRiM experience suggested to develop a full six-components hexapod-design prototype of MFT. In fact, calibration results showed that the measurement of F_x is not affected only by the value of $F_{m,x}$, but also by $M_{m,x}$ and the interaction term $F_{m,x} \cdot F_{m,z}$.

Besides, the uncertainty associated to the values of transversal and axial force was evaluated. The applied calibration method confirmed these uncertainty values to be well within customer specified targets, a relative expanded uncertainty of about 0.2% being obtained for both the transversal force and the corresponding value of the axial force. The latter is definitely within class 1 requirements of ISO 7500-1:2004.

References

- Trenitalia, "Specifica tecnica di fornitura di molle ad elica per sospensioni di rotabili ferroviari", Specifica n. 307625 esp. 05, Roma, 2010 (in Italian).
- [2] G. Barbato, S. Desogus, A. Germak, Calibration system for multicomponent force and moment transducers, Exp. Mech. (1992) 341-352.
- [3] A. Bray, G. Barbato, R. Levi, Theory and Practice of Force Measurement, Academic Press, London, 1989.
- [4] M. Sorli, S. Pastorelli, Six-axis reticulated structure force/torque sensor with adaptable performances, Mechatronics 5 (6) (1995) 585-601.
- [5] Y. Hou, J. Yao, L. Lu, Y. Zhao, Performance analysis and comprehensive index optimization of a new configuration of Stewart six-component force sensor, Mech. Mach. Theory 44 (2009) 359–368.
- [6] ISO 7500-1:2004, Metallic materials verification of static uniaxial testing machines – Part 1: Tension/compression testing machines – verification and calibration of the force-measuring system.

- [7] S. Desogus, A. Germak, F. Mazzoleni, D. Quagliotti, G. Barbato, A. Barbieri, G. Bigolin, C. Bin, Developing multicomponent force transducers at INRiM, in: Proceedings of the IMEKO 2010 TC3, TC5 and TC22 Conferences, Metrology in Modern Context, Pattaya, Chonburi, Thailand, November 2010.
- [8] JCGM 100:2008, Evaluation of measurement data guide to the expression of uncertainty in measurement (GUM).
- [9] ISO 376:2011, Metallic materials calibration of force proving instruments used for the verification of uniaxial testing machines.
- [10] N.R. Draper, H. Smith, Applied Regression Analysis, second ed., Wiley, New York, 1981.
- [11] R.R. Hocking, The analysis and selection of variables in linear regression, Biometrics 32 (1976) 1–49.
- [12] G. Genta, Methods for Uncertainty Evaluation in Measurement, VDM Verlag, Saarbrücken, 2010.
- [13] G. Barbato, A. Germak, G. Genta, Measurements for Decision Making, Società Editrice Esculapio, Bologna, 2013.
- [14] ISO 14253-2:2011, Geometrical product specifications (GPS) inspection by measurement of workpieces and measuring equipment Part 2: Guidance for the estimation of uncertainty in GPS measurement, in calibration of measuring equipment and in product verification.
- [15] EA-4/02 M:2013, Evaluation of the uncertainty of measurement in calibration.